ChemComm

COMMUNICATION

View Article Online
View Journal | View Issue

Cite this: *Chem. Commun.*, 2020, **56**, 8063

Received 3rd April 2020,
Accepted 29th May 2020

DOI: 10.1039/d0cc02408b

rsc.li/chemcomm

Capture and identification of coke precursors to elucidate the deactivation route of the methanol-to-olefin process over H-SAPO-34†

Bowen Yu,‡[ab] Wenna Zhang,‡[a] Yingxu Wei,*[a] Xinqiang Wu,[a] Tantan Sun,[ab] Benhan Fan,[ab] Shutao Xu [a] and Zhongmin Liu *[a]

The evolution of retained species during the whole methanol-to-olefins process was revealed with the aid of GC-MS, thermogravimetric analysis (TG) and density functional theory (DFT) calculations. Precise routes for the transformation of retained methylbenzenes to methylnaphthalenes were proposed, based on the direct capture of three possible organic intermediates, to explain the catalyst deactivation procedure.

The methanol-to-olefins (MTO) process has been considered one of the most successful non-petrochemical routes to produce light olefins, ethene and propene, the chemicals that constitute the backbone of the petrochemical industry. In 2010, the world's first commercial MTO plant was successfully constructed in Baotou, China, employing the DMTO process developed by the Dalian Institute of Chemical Physics. By employing SAPO-34 molecular sieves as catalysts with unique small pore opening and chabazite (CHA) cage structures, high methanol conversion and relatively high light olefin selectivity were realized.[1–3]

As an important area of MTO study, the mechanism of methanol-to-olefins has been studied extensively to provide guidance for both fundamental research and industrial applications over the past four decades.[2–7] Achievements have been gained for the first C–C bond formation *via* a direct mechanism[4,5,8–11] in the early stage, and olefin production *via* an indirect mechanism[12–19] in the steady-state stage using experimental evidence and theoretical calculation of the MTO reaction. According to the accepted indirect mechanism, methanol that reacts on the hydrocarbon pool (HCP) species,[14–18] such as polymethylbenzenes and polymethylcyclopentadienes, was retained in the catalysts and olefins were split off from these active species. The aging and transformation of these active species to polymethylnaphthalenes and polycyclic aromatic hydrocarbons causes deactivation, with the occurrence of pore blockage and the acid site coverage of the catalysts.[20–25]

Study of the formation of deactivation species is important for understanding the MTO reaction and catalyst deactivation. Han proposed that oxygen-containing coke species are one of the precursors that can be converted to aromatics and coke species on H-ZSM-5.[26] Bjørgen and co-workers[23] found that dihydrotrimethylnaphthalene, as the precursor of naphthalene derivatives, can be produced from heptamethylbenzenium (heptaMB$^+$) by hydrogen transfer and molecular rearrangement. Sassi[20] also observed trace amounts of tetrahydro-1,4-dimethylnaphthalene when co-feeding of methanol and methylbenzenes was adopted, and speculated that it could be formed by coupling two isopropyl groups that are located *ortho* to each other on the benzene ring. From calculation results, Hemelsoet[27,28] proposed that the growth of naphthalenic compounds within a zeolite with chabazite topology is energetically feasible through successive methylation reactions. However, the detailed mechanism and experimental evidence of the transformation of methylbenzenes to methylnaphthalenes was not very clear, and detailed elementary reactions for formation of methylnaphthalenes, as the key step for the transformation of reactive HCP species to coke species, needs further exploration and more detailed elucidation. Such an understanding of the evolution of organic species would provide a strategy for controlling the MTO reaction.

In this contribution, methanol conversion was performed on H-SAPO-34 at 350 °C with a high weight hourly space velocity (WHSV) of methanol to obtain a whole view of the methanol conversion during the induction period, steady-state period and deactivation period. We monitored the evolution of retained organic species and their variation in activity during methanol conversion. The evolution of organic species over H-SAPO-34 was

[a] *National Engineering Laboratory for Methanol to Olefins, Dalian National Laboratory for Clean Energy, iChEM (Collaborative Innovation Center of Chemistry for Energy Materials), Dalian Institute of Chemical Physics, Chinese Academy of Sciences, Dalian 116023, P. R. China. E-mail: weiyx@dicp.ac.cn, liuzm@dicp.ac.cn*

[b] *University of Chinese Academy of Sciences, Beijing 100049, P. R. China*

† Electronic supplementary information (ESI) available. See DOI: 10.1039/d0cc02408b

‡ B. Yu and W. Zhang contributed equally to this work.

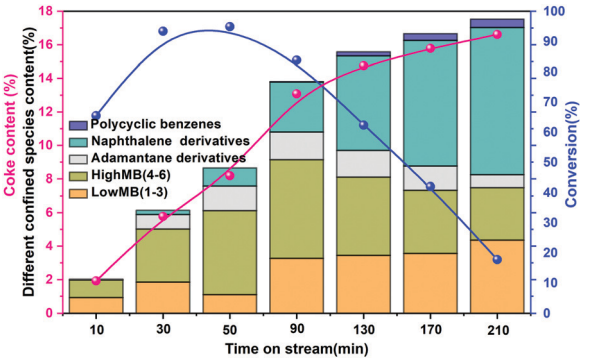

Fig. 1 Methanol conversion and the evolution of retained organic species with time on a stream over H-SAPO-34 at 350 °C and WHSV of 6 h^{-1}.

correlated to the three stages of methanol conversion. In particular, intermediates for possible transformation of methylbenzenes to methylnaphthalenes were captured, which gave direct evidence of aging of the reactive HCP species for the naphthalene derivatives with lower reactivity. Meanwhile DFT calculation demonstrated the feasibility of the transformation of methylbenzenes to methylnaphthalenes.

The results for the characterization of H-SAPO-34 are given in the ESI† (Fig. S1–S4). The methanol-to-olefin reaction was performed on H-SAPO-34 with a Si molar content of 0.06 ($n_{Si}/n_{Si} + n_{Al} + n_P$ = 0.06 (in mole ratio)) at 350 °C and WHSV = 6 h^{-1}. Mild reaction conditions and the use of a catalyst with relatively low acid density ensure accurate observation and tracing of the evolution of the MTO reactions and generation of the retained organic species. The variation of methanol conversion with coke formation, as presented in Fig. 1, made it possible to divide the whole reaction course into three reaction stages: an induction period from 0 to 50 min, an efficient reaction period from 50 to 90 min and a deactivation period from 130 to 210 min. A rational relationship between methanol conversion and confined organics evolution in the catalyst with time-on-stream (TOS) can be clearly established. When the coke species accumulated in the early stage, the conversion of methanol increased sharply to almost 100% conversion at 50 min. At the beginning of the reaction, from 10 to 50 min, the amount of retained organic species increased from 2 to 8.6 wt%, accompanied by an increase in the methanol conversion from 65.42% to 94.89%. After methanol conversion hit a peak at 50 min, further coke deposition gave rise to a reverse trend for methanol conversion. The weight of the coke increased to 17.53 wt% at TOS of 210 min, while methanol conversion declined to 17.75%. Product selectivity also varied with coke formation. Selectivity of ethene increased from 18.9% to 27.1%, while that of propene decreased from 48.6% to 42.9% with the amount of coke increasing from 2.03 wt% to 17.53 wt% (Fig. S5, ESI†). Moreover, the ^{13}C-NMR signals of the retained organic species exhibit the same evolving trends with TOS (Fig. S6, ESI†).

In combination with TG analysis, ^{13}C-NMR and GC-MS analysis after catalyst dissolution in HF solution and extraction of the retained organics with CH_2Cl_2, the detailed evolution with reaction time of the five types of organic species confined in the H-SAPO-34 catalyst was determined. The different trends are shown in Fig. 1, corresponding to the methanol reaction during the three reaction stages. At the beginning of the reaction, polymethylbenzene formation in the catalyst and the concentration increase of the active HCP species gave rise to the enhancement of methanol conversion during the initial 50 min. At the same time, adamantane hydrocarbons and methylnaphthalene derivatives, also increased in intensity, but at a lower level compared to the methylbenzenes. When the reaction time was prolonged to 90 min, the quantity of methylbenzenes, especially polymethylbenzenes, started to decrease, while that of methylnaphthalenes increased sharply to a relatively high level and became the dominating coke species. This change of organic species was accompanied by the decline in methanol conversion from a TOS of 50 min. In the deactivation period (170 min and 210 min), methylnaphthalenes dominated among the retained organic species in the catalyst, and accounted for approximately 50% of the coke species. It is noteworthy that methylnaphthalenes increased over the whole reaction period. After the induction period, with the polymethylbenzenes decreasing in intensity, lower methylbenzene formation was also achieved. In addition, a small amount of adamantane hydrocarbons and polyaromatic hydrocarbons appeared amongst the coke species, and their intensity increased slightly with reaction time. These results illustrate that the both improvement or depression of methanol conversion are associated with variation in the nature and quantity of coke. The reaction mechanism from the highly efficient stage to the deactivation period is critical for development of the methanol reaction process. Therefore, in the following section, transformation of the active species (methylbenzenes) to coke species (methylnaphthalenes) was investigated in detail based on direct capture of the organic intermediates.

The coke analysis described above indicated that among the retained organic species of methanol reaction over H-SAPO-34, the decrease in polymethylbenzenes was accompanied by an increase in polyaromatics, such as methylnaphthalenes, phenanthrene and pyrene, during the deactivation period. This implied that the initially formed methylbenzenes in the catalyst would convert to methylnaphthalenes and polycyclic aromatics during the deactivation period, but how methylbenzenes transform to methylnaphthalenes on H-SAPO-34 catalysts still remains unclear. In this work, the confined organics in the catalyst of methanol conversion were analyzed thoroughly and the intermediates or precursors for formation of methylnaphthalenes under real reaction conditions were successfully captured. Based on this evidence, a rational route for the transformation of methylbenzenes to methylnaphthalenes is proposed.

The organic species confined in the H-SAPO-34 catalyst after methanol conversion for 130 min were analyzed by GC-MS, as shown in Fig. 2. Besides the abundant retained compounds, such as methylbenzenes and methylnaphthalenes, three organic species in relatively low intensity were successfully captured after methanol conversion for 130 min, which were possibly the important precursors of methylnaphthalenes. The peaks with retention times of 18.7, 20.7 and 23.45 min were assigned to

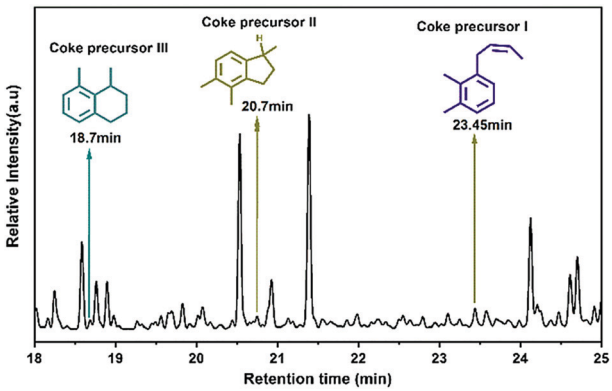

Fig. 2 Capture and identification of the intermediates by GC-MS after methanol conversion over H-SAPO-34 catalysts for 130 min.

tetrahydro-1,8-dimethylnaphthalene, dihydro-1,5,6-trimethly-1*H*-indene and 1,2-dimethyl-3-(2-butenyl)benzene, or their possible isomers, on the basis of the NIST-11 database. Two possible routes for the formation of 1,2-dimethylnaphthalene from methylbenzenes with the involvement of these three intermediates are further depicted in Scheme 1.

As described in Scheme 1, starting from 1,2-dimethyl-3-(2-butenyl)benzene (**coke precursor I**), its isomerized compounds, 1,2-dimethyl-4-(1-methyl-2-propenyl)benzene (**coke precursor I′**) and 1,2-dimethyl-4-(3-butenyl)benzene (**coke precursor I″**) are first protonated over H-SAPO-34 to form the corresponding carbenium ions. Then, the carbenium ions possibly convert to 1, 2-dimethylnaphthalene by means of route 1 or route 2. For route 1, **coke precursor I′** is protonated and transformed to **coke precursor II** (dihydro-1,5,6-trimethly-1*H*-indene) *via* a cyclization reaction, and, subsequently, the protonated form of **coke precursor II** transforms into 1,2-dimethylnaphthalenecarbenium by hydrogen transfer, dehydrogenation, ring-enlargement and deprotonation reactions. In route 2, tetrahydro-1,2-dimethylnaphthalene (**coke precursor III**) can be generated from **coke precursor I″** by protonation, hydrogen transfer, cyclization and deprotonation reactions. After that, olefins (ethene, propene, butene) can be produced from the coke species *via* an elimination reaction by means of route 3.

Here, the critical steps, such as cyclization and ring enlargement, for the formation of dimethylnaphthalene from the **coke precursors I′** and **I″** were used to evaluate the feasibility of route 1 and route 2 over the H-SAPO-34 model (Fig. S7, ESI†) using theoretical calculations. The isomerization,[29,30] deprotonation[31] and hydrogen transfer reactions needed to overcome a relatively low energy barrier in the MTO reaction catalyzed on cage-type catalysts in previous studies. The calculated Gibbs free energy barriers at 623 K and the transition state structures of the critical steps are presented in Scheme 1. For route 1, the free energy barriers for the cyclization and ring-enlargement reactions are 21.42 and 19.29 kcal mol^{-1}, with reaction rate constants of 8.20×10^4 and 6.23×10^5 s^{-1}, respectively. The cyclization reaction in route 2 presents a free energy barrier of 10.30 kcal mol^{-1} at a temperature of 623 K, which is 9.0–11.12 kcal mol^{-1} lower than the reactions in route 1, and the rate constant of 2.21×10^9 s^{-1} is 4–5 orders of magnitude higher than that in route 1. Therefore, although, rationally, both routes could generate 1,2-dimethylnaphthalene, route 2 is more energetically favorable than route 1 for the formation of 1,2- dimethylnaphthalene. However, it is noteworthy that splitting off propene from 1,2-dimethyl-4-(3-butenyl)-benzene through the elimination reaction in route 3 needs to overcome a higher free energy barrier of 33.61 kcal mol^{-1}, with a lower reaction rate constant (5.48×10^0 s^{-1}) than other two routes. The energy barrier of the elimination reaction in route 3 to form propene products is higher than that of the cyclization steps in route 1 and 2 to form the precursors of the naphthalene derivatives. Thus, the **coke precursors I′** and **I″** tend to form

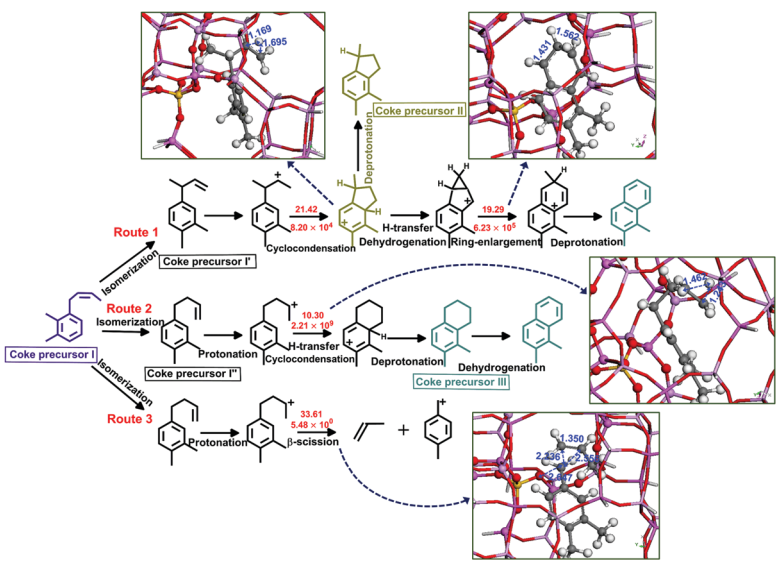

Scheme 1 The possible routes of coke precursor evolution over H-SAPO-34. Calculated free energy barriers and reaction rate constants at 350 °C are given in kcal mol^{-1} and s^{-1}, respectively. Optimized transition state structures of these critical steps are presented near the corresponding reaction.

1,2-dimethylnaphthalene rather than produce propene. Therefore, on the basis of capture of a series of possible intermediates observed in the real MTO reaction, different transformation routes of methylbenzenes to methylnaphthalenes are proposed.

Methylbenzenes with bulky alkyl side chain, such as 1,2-dimethyl-3-(2-butenyl)benzene, usually work as the precursor for alkene products, with butenes and other alkenes generated *via* an elimination reaction. During the deactivation period, with much more confined generation and accumulation of organic species, the reactivity of the catalyst declined and the elimination reaction could not be efficiently realized. At the same time, mass transfer reduction also limited the diffusion of some higher hydrocarbons out of the catalyst crystal, especially C_4^+ olefins generated in the catalyst. Some side reactions, including isomerization (H/CH_3 transfer) and cyclization of benzenes with bulky side chains, may generate coke precursors, such as methylindene and tetrahydro-methylnaphthalene in the supercage of H-SAPO-34, leading to the transformation of methylbenzene to polyaromatics. This evolution of confined organics finally gives rise to severe deactivation of the catalyst due to occupation of the CHA cavities of SAPO-34 by the inert aromatic hydrocarbon coke species.

In conclusion, with the aid of GC-MS, TG analysis and DFT calculations, the evolution of retained species on reaction and deactivation during the whole MTO process was successfully clarified. At the beginning of the MTO reaction over H-SAPO-34 catalyst, polymethylbenzenes as the active intermediates were formed and accumulated during the induction period, which accounted for the highly efficient methanol conversion during the steady-state reaction period. However, during the deactivation period, polymethylbenzenes gradually transformed to methylnaphthalenes, which played a decisive role in the deactivation of the MTO reaction. Two possible routes for the evolution of methylbenzenes to methylnaphthalenes are proposed based on the first-time capture of three key intermediate species, tetrahydro-1,8-dimethylnaphthalene, dihydro-1,5,6-trimethyl-1*H*-indene, and 1,2-dimethyl-3-(2-butenyl)benzene and their possible isomers, as the precursors of naphthalene derivatives. Theoretical calculation confirmed the feasibility of these routes. When alkylbenzenes with bulky side chains were formed, both olefin generation and methylnaphthalene formation possibly occurred, while the predominance of the reaction route depended on the different stage of the methanol conversion reaction. The low energy barrier of methylnaphthalene formation and high energy barrier of propene elimination in the reaction network of confined organics transformation makes deactivation an inevitable trend. Slowing the evolution of active species for coke deposits, as a strategy to prolong the lifetime of the SAPO-34 catalyst, is of great importance for the industrial MTO process.

This work was supported by the National Natural Science Foundation of China (No. 21991090, 21991092, 91745109 and 21972142), the Key Research Program of Frontier Sciences, Chinese Academy of Sciences (QYZDY-SSW-JSC024), the International Partnership Program of Chinese Academy of Sciences (121421KYSB20180007) and the Strategic Priority Research Program of the Chinese Academy of Sciences (XDA21030200).

Conflicts of interest

There are no conflicts to declare.

References

1 P. Tian, Y. Wei, M. Ye and Z. Liu, *ACS Catal.*, 2015, **5**, 1922–1938.
2 U. Olsbye, S. Svelle, M. Bjorgen, P. Beato, T. V. W. Janssens, F. Joensen, S. Bordiga and K. P. Lillerud, *Angew. Chem., Int. Ed.*, 2012, **51**, 5810–5831.
3 S. Xu, Y. Zhi, J. Han, W. Zhang, X. Wu, T. Sun, Y. Wei and Z. Liu, *Adv. Catal.*, 2017, **61**, 37–122.
4 M. StÖcker, *Microporous Mesoporous Mater.*, 1999, **29**, 3–48.
5 I. Yarulina, A. D. Chowdhury, F. Meirer, B. M. Weckhuysen and J. Gascon, *Nat. Catal.*, 2018, **1**, 398–411.
6 J. F. Haw, W. G. Song, D. M. Marcus and J. B. Nicholas, *Acc. Chem. Res.*, 2003, **36**, 317–326.
7 D. Chen, K. Moljord and A. Holmen, *Microporous Mesoporous Mater.*, 2012, **164**, 239–250.
8 W. G. Song, D. M. Marcus, H. Fu, J. O. Ehresmann and J. F. Haw, *J. Am. Chem. Soc.*, 2002, **124**, 3844–3845.
9 H. Yamazaki, H. Shima, H. Imai, T. Yokoi, T. Tatsumi and J. N. Kondo, *Angew. Chem., Int. Ed.*, 2011, **50**, 1853–1856.
10 A. D. Chowdhury, K. Houben, G. T. Whiting, M. Mokhtar, A. M. Asiri, S. A. Al-Thabaiti, S. N. Basahel, M. Baldus and B. M. Weckhuysen, *Angew. Chem., Int. Ed.*, 2016, **55**, 15840–15845.
11 X. Q. Wu, S. T. Xu, W. N. Zhang, J. D. Huang, J. Z. Li, B. W. Yu, Y. X. Wei and Z. N. Liu, *Angew. Chem., Int. Ed.*, 2017, **56**, 9039–9043.
12 I. M. Dahl and S. Kolboe, *J. Catal.*, 1994, **149**, 458–464.
13 I. M. Dahl and S. Kolboe, *J. Catal.*, 1996, **161**, 304–309.
14 J. F. Haw, J. B. Nicholas, W. G. Song, F. Deng, Z. K. Wang, T. Xu and C. S. Heneghan, *J. Am. Chem. Soc.*, 2000, **122**, 4763–4775.
15 W. G. Song, J. F. Haw, J. B. Nicholas and C. S. Heneghan, *J. Am. Chem. Soc.*, 2000, **122**, 10726–10727.
16 M. Bjorgen, S. Svelle, F. Joensen, J. Nerlov, S. Kolboe, F. Bonino, L. Palumbo, S. Bordiga and U. Olsbye, *J. Catal.*, 2007, **249**, 195–207.
17 C. Wang, J. Xu, G. D. Qi, Y. J. Gong, W. Y. Wang, P. Gao, Q. Wang, N. D. Feng, X. L. Liu and F. Deng, *J. Catal.*, 2015, **332**, 127–137.
18 S. Xu, A. Zheng, Y. Wei, J. Chen, J. Li, Y. Chu, M. Zhang, Q. Wang, Y. Zhou, J. Wang, F. Deng and Z. Liu, *Angew. Chem., Int. Ed.*, 2013, **52**, 11564–11568.
19 W. Zhang, Y. Zhi, J. Huang, X. Wu, S. Zeng, S. Xu, A. Zheng, Y. Wei and Z. Liu, *ACS Catal.*, 2019, **9**, 7373–7379.
20 A. Sassi, M. A. Wildman, H. J. Ahn, P. Prasad, J. B. Nicholas and J. F. Haw, *J. Phys. Chem. B*, 2002, **106**, 2294–2303.
21 J. Zhong, J. Han, Y. Wei, S. Xu, T. Sun, X. Guo, C. Song and Z. Liu, *Chin. J. Catal.*, 2018, **39**, 1821–1831.
22 A. Sassi, M. A. Wildman and J. F. Haw, *J. Phys. Chem. B*, 2002, **106**, 8768–8773.
23 M. Bjorgen, U. Olsbye and S. Kolboe, *J. Catal.*, 2003, **215**, 30–44.
24 Z. Wei, Y.-Y. Chen, J. Li, P. Wang, B. Jing, Y. He, M. Dong, H. Jiao, Z. Qin, J. Wang and W. Fan, *Catal. Sci. Technol.*, 2016, **6**, 5526–5533.
25 J. Zhong, J. Han, Y. Wei, S. Xu, T. Sun, S. Zeng, X. Guo, C. Song and Z. Liu, *Chin. J. Catal.*, 2019, **40**, 477–485.
26 Z. Liu, X. Dong, X. Liu and Y. Han, *Catal. Sci. Technol.*, 2016, **6**, 8157–8165.
27 K. Hemelsoet, A. Nollet, M. Vandichel, D. Lesthaeghe, V. Van peybroeck and M. Waroquier, *ChemCatChem*, 2009, **1**, 373–378.
28 K. Hemelsoet, A. Nollet, V. Van Speybroeck and M. Waroquier, *Chem. – Eur. J.*, 2011, **17**, 9083–9093.
29 D. Lesthaeghe, J. Van der Mynsbrugge, M. Vandichel, M. Waroquier and V. V. Speybroeck, *ChemCatChem*, 2011, **3**, 208–212.
30 C.-M. Wang, Y.-D. Wang and Z.-K. Xie, *J. Catal.*, 2013, **301**, 8–19.
31 K. De Wispelaere, K. Hemelsoet, M. Waroquier and V. V. Speybroeck, *J. Catal.*, 2013, **305**, 76–80.

